7

Pinching Effort Evaluation Based on Tendon Force Estimation

Atsutoshi Ikeda, Yuichi Kurita and Tsukasa Ogasawara
Nara Institute of Science and Technology
Japan

1. Introduction

The quantitative evaluation of product usability is important for product design. Most products, e.g. digital cameras, remote controls, and cellphones, have holding and operation parts where the hands are placed. The pinching effort which is the feeling when an user picks up and controls a product is important for product usability. Demands for product design that considers the pinching effort have increased. However, quantitative evaluation of sensibility is difficult. A questionnaire survey using a semantic differential method is commonly used for the subjective evaluation of the usability. In recent years, quantitative evaluation methods have been proposed based on physical data that are measurable by sensors. Radhakrishnan & Nagaravindra (1993) analyzed the force distribution during grasping a tube. Kong & Freivalds (2003) measured the maximum pulling force, the surface EMG (electromyogram), and the contact force, when pulling seven different meat hooks. They also developed a biomechanical hand model to estimate the tendon force. These research methods addressed the quantitative evaluation of a power grasp using the whole hand (palm and fingers).
On the other hand, some research methods in biomechanics have proposed an accurate musculoskeletal model of the human hand and fingers; An et al. (1979) established a three-dimensional normative hand model based on X-ray image analysis. Brook et al. (1995) introduced a dynamic index finger model using a set of moment arm coefficients and elongation equations. Sueda et al. (2008) developed a method for generating motions of tendons and muscles for hand animation. Holzbaur et al. (2005) developed a biomechanical model of the upper extremity, Flanagan et al. (2006) discussed control strategies of the human fingertips, Valero-Cuevas (2005) proposed a detailed model of the human finger, including neuro-musculo-skeletal interactions. Also, in robotics, there have been a lot of research methods related to skin and muscle modeling. For example, Nakamura et al. (2005) proposed a computation method of somatosensory information from motion-capture data. Tada & Pai (2008) developed a simple finger shell model that is efficient to quickly simulate the finger surface deformation. However, these research methods were not applied to the quantitative evaluation of product usability.
A goal of this research is to design an evaluation system of product usability using a simulation in conjunction with multiple sensors, such as contact sensors, pressure sensors, and force sensors. Fig. 1 shows the concept of the evaluation system, which is designed to correlate the obtained sensor data with the human sensory information. Ikeda et al. (2008) has

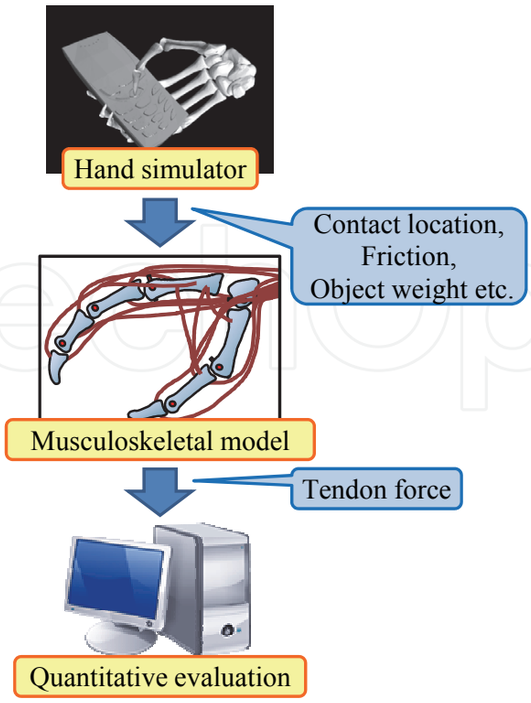

Fig. 1. Concept of the evaluation system

presented the concept of the evaluation of the pinching effort. We (Ikeda et al. (2009a) and Ikeda et al. (2009b)) have also evaluated the usability in the pinching activity by comparing the sensor data from the sensing hand with the human muscle activity.

In this chapter, we discuss the relationship between the pinching effort and the EMG data. Then we propose the evaluation method of the pinching effort using a tendon skeletal finger model. At the beginning of this chapter, the human pinching activity is analyzed to show that the tendon force reflect well the human sensation. Since we can not directly measure the tendon force in humans, we measure the surface EMG instead of the tendon force and compare the surface EMG with the questionnaire results in the human experiment. Second, we describe the detail of the tendon skeletal finger model and the pinching effort evaluation method. The score of pinching effort is calculated from the tendon forces which are estimated in a pinching simulation. The simulation result is compared with the human experiment result. These results show that the proposed method is useful for the quantitative evaluation of the pinching effort.

2. Human pinching experiment

2.1 Measurement system

Fig. 2 shows an overview of the experiment to measure human pinching activity. A capacitance triaxial kinesthetic sensor (PD3-32-05-80, Nitta) was put inside a holding cylinder to measure the pinching force. Disposable radiolucent electrodes (F-150S, Nihon Kohden) were put on the hand and the arm of the subject to measure the surface EMG of the FDS (flexor digitorum superficialis) muscle and the ADP (adductor pollicis muscle). The FDS muscle flexes the PIP joint of the index finger, and the ADP muscle adducts the CMC joint of the

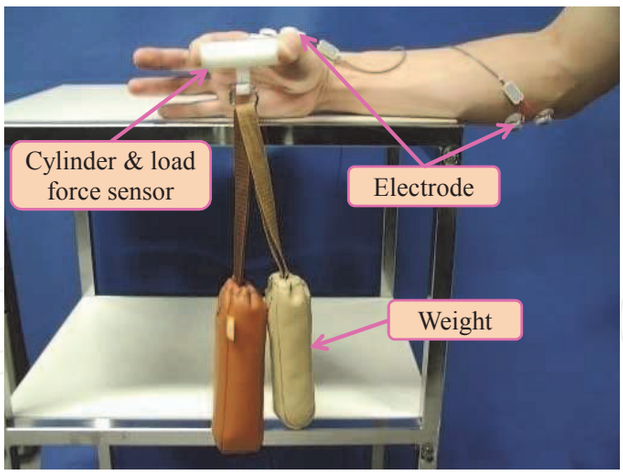

Fig. 2. Experiment overview of pinching an object

thumb. Fig. 3 shows the normal location of muscles in the forearm and the hand. The surface EMG were amplified by an EMG amplifier (EMG-021, Harada Electronics Industry) and stored in a PC through an A/D board (CSI-360116, Interface). In this chapter, the following processes are used for a quantitative analysis of the EMG signal:

1. Detrending: Remove, the DC (direct current) offset from the raw EMG signal
2. Rectification: Translates the EMG signal, that have been removed of the DC offset, to a positive polarity
3. Filtering: Smooth the rectified EMG signal using a low-pass filter ($4[Hz]$)
4. Integration: Calculate the integration value of the filtered EMG.
5. Normalization: Normalize the integrated EMG (EMG_{intg}) using a maximum/minimum EMG (EMG_{max} and EMG_{min}) value which are preliminary measured:

$$EMG_{norm} = \frac{EMG_{intg} - EMG_{min}}{EMG_{max} - EMG_{min}} + 1 \tag{1}$$

Fig. 4 shows the cylinders used in the experiment. These cylinders are made of ABS (acrylonitrile butadiene styrene) resin. Dimension of the cylinders are 20, 40, 60, 80 and 100 [mm] in length and 20 [mm] in diameter.

2.2 Experimental method

In our experiment, 300 and 600 [g] weights were used. Five healthy male subjects, average age: 24 years old and SD: 3.4, volunteered for the experiment. All subjects were given the experimental detail and they gave their consent to participate. The pinching activity was performed with their dominant arm. The arm of the subject was placed on a desk, and the middle, ring, and pinky finger were kept open so as not to influence the pinching activity. Subjects pinch in the length direction of the cylinder by using the index finger and thumb. Table 2 shows the average and standard deviation of the subjects' hand sizes. Fig. 5 shows the definition of the measured dimensions of the hand. The subjects' hand sizes were similar to the standard Japanese hand size.

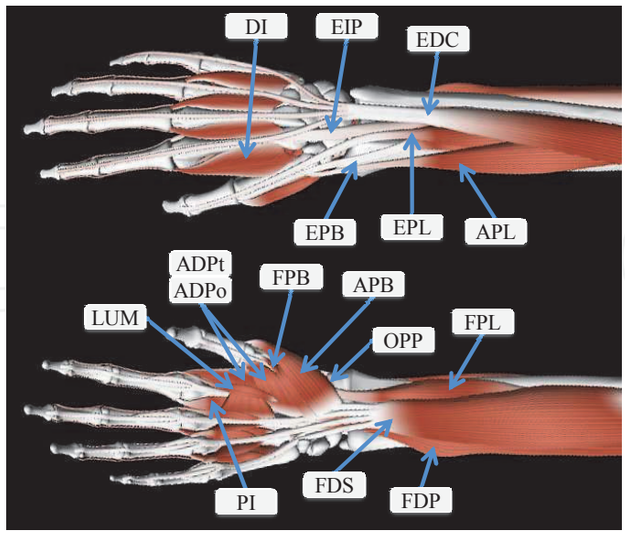

Fig. 3. Muscles that drive the index finger and the thumb (This figure is drawn with Kaitai Ensyo (gsport,inc.))

Index finger	
FDP	Flexor Digitorum Profundus
FDS	Flexor Digitorum Superficialis
EIP	Extensor Indicis Proprius
EDC	Extensor Digitorum Proprius
LUM	Lumbricalis
DI	Dorsal Interosseous
PI	Palmar Interosseous
Thumb	
FPL	Flexor Pollicis Longus
FPB	Flexor Pollicis Brevis
EPL	Extensor Pollicis Longus
EPB	Extensor Pollicis Brevis
APL	Abductor Pollicis Longus
APB	Abductor Pollicis Brevis
ADPt	The Transverse Head of The Adductor Pollicis
ADPo	The Oblique Head of The Adductor Pollicis
OPP	Opponents Pollicis

Table 1. List of muscle in the hand and the fore arm

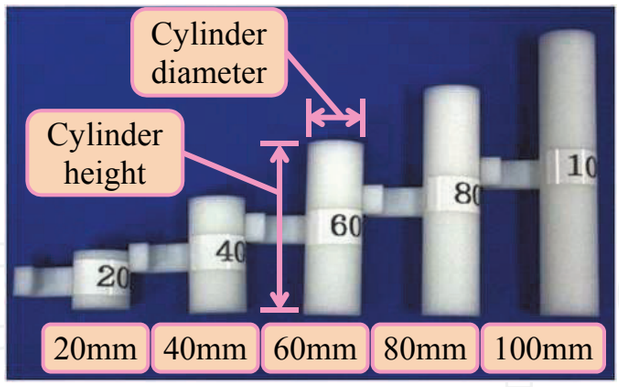

Fig. 4. Cylinder dimensions

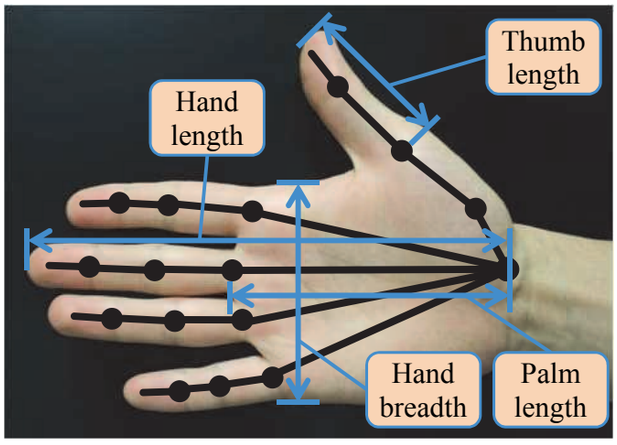

Fig. 5. Measured dimensions (see definitions of measurement on the website of Digital Human Research Center, AIST (http://www.dh.aist.go.jp/))

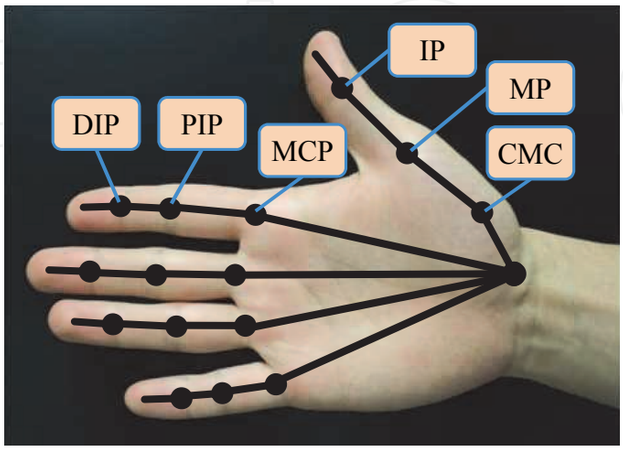

Fig. 6. Joint name of the index finger and the thumb

Before beginning the experiment, we explained its purpose to the subjects. In the experiment, the subjects pinched each cylinder and scored the effort level of the cylinder. The score had five levels from 1: "very easy to pinch" to 5: "very difficult to pinch". The subjects pinch the cylinders in arbitrary order and hold the cylinders for 15 [sec]. A two-minute interval was taken between each trial.
The subjects joint angles when pinching each cylinder was measured using a CyberGlove (CyberGlove Systems LLC). Fig. 6 shows the joint notation of the index finger and the thumb. We measure eight angles: the MCP (metacarpophalangeal: in the index finger) joint FE (flexion/extension direction), the MCP joint AA (adduction/abduction direction), the PIP (proximal interphalangeal) joint FE, the DIP (distal interphalangeal) joint FE, the CMC (carpometacarpal) joint FE, the CMC joint AA and the MP (metacarpophalangeal: in the thumb) joint FE. We can not measure the MP joint AA and the IP (Interphalangeal) joint FE because sensors were not present in the CyberGlove. The human joint angles are compared with simulation results.

2.3 Human experimental results

2.3.1 Questionnaire survey results

Fig. 7 shows the average and standard deviation of the scores. The curves in the figure are the approximate quadratic curves of the 300 and 600 [g] weights. The lowest score is observed in the 60 [mm] cylinder length for both the 300 and 600 [g] weights. On the other hand, higher score is observed when the cylinder length is 20 and 100 [mm] for both the 300 and 600 [g] weights. A possible reason is that the finger posture when pinching the middle length cylinder makes it easier to exert a pinching force.

2.3.2 Pinching force measurement results

Fig. 8 shows the typical pinching force when a subject pinches a cylinder. The dash line and the dot-dash line in the figure designate the theoretical force necessary to pinch the cylinders with 300 and 600 [g] weight, respectively. The theoretically necessary forces F_{theo} are calculated based on the friction coefficient μ between the finger and the cylinder:

$$F_{theo} = \mu M_{obj} \tag{2}$$

where M_{obj} is the weight of the object and $\mu = 0.5$. The measured force is somewhat larger than the theoretically necessary force because a human applies a safety margin in order to pinch an object tightly.
The highest pinching force is observed when a subject pinches the 100 [mm] cylinder for both weights. The possible reason is that the 100 [mm] is the hardest to pinch.

	Ave.	SD
Hand length [mm]	184.4	5.5
Palm length [mm]	104.6	4.7
Hand breadth [mm]	82.6	5.3
Thumb length [mm]	61.6	2.8

Table 2. Average and standard deviation of hand size (see definitions in Fig. 5)

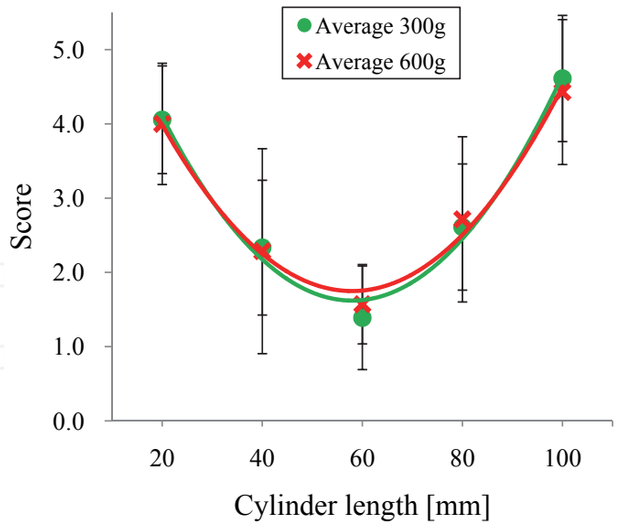

Fig. 7. Questionnaire results

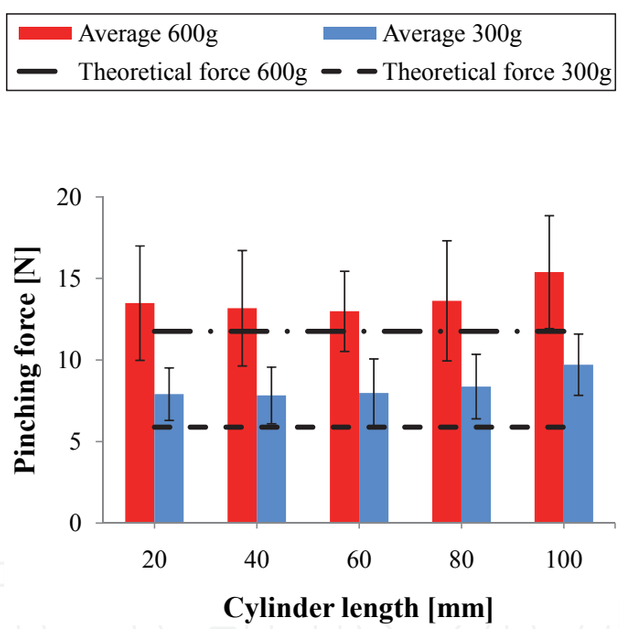

Fig. 8. Pinching force

2.3.3 Surface EMG measurement results

We evaluate the pinching effort from the EMG signal during the pinching activity. The EMG signal is normalized using the data process, shown in Sec. 2.1, because the amplitudes of the EMG signals are different between each subject.

Fig. 9 shows the normalized EMG related to the index finger and thumb when the cylinder weight is 300 [g], and Fig. 10 shows the normalized EMG when the cylinder weight is 600 [g]. The normalized EMG of the index finger FDS becomes lower according to the cylinder length, and the normalized EMG of the thumb ADPt becomes higher according to the cylinder length. The possible reason is that the finger posture when pinching a short cylinder makes it hard for

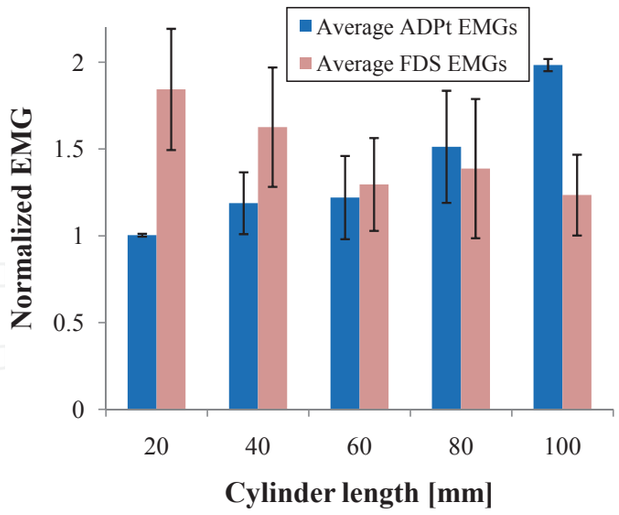

Fig. 9. Integrated EMG (300[g])

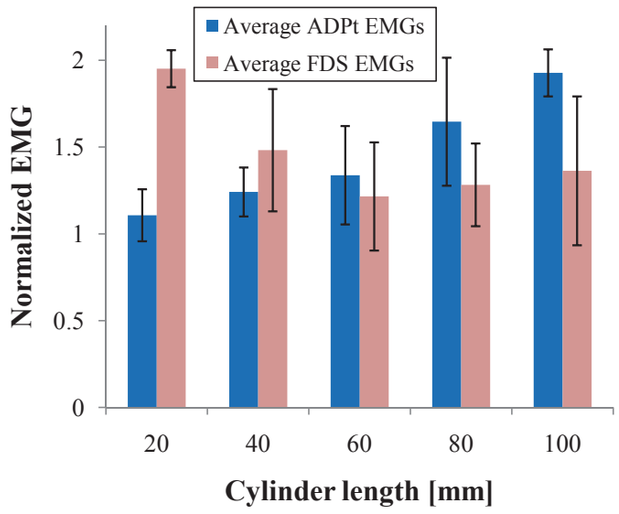

Fig. 10. Integrated EMG (600[g])

the index finger to exert a pinching force. On the other hand, when pinching a long cylinder, a large antagonist force is necessary to open the thumb widely, and thus the muscle activity of the thumb increases.

Fig. 11 shows the average EMG and the questionnaire score when the cylinder weight is 300 [g], and Fig. 12 shows the average EMG and the questionnaire score when the cylinder weight is 600 [g]. The lowest score is observed when the subject pinches the cylinder with the lowest EMG, and the highest score is observed when the subject pinches the cylinder with the highest EMG. The correlation coefficients between the average EMG and the questionnaire result are 0.86 at 300 [g] and 0.97 at 600 [g]. The p-values are 0.061 at 300 [g] and 0.005 at 600 [g]. Thus there are correlations between the surface EMG and the questionnaire result, but the p-value of 300 [g] result is high ($p > 0.05$). A possible reason is that the 300 [g] weight was too light to evaluate the pinching effort. These results signify that the integrated surface EMG is an important index to indicate pinching effort, pointing to the potential for

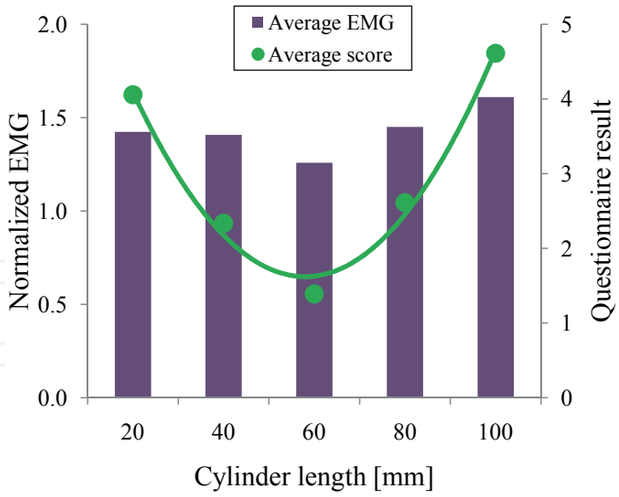

Fig. 11. Average EMG and questionnaire score (300[g])

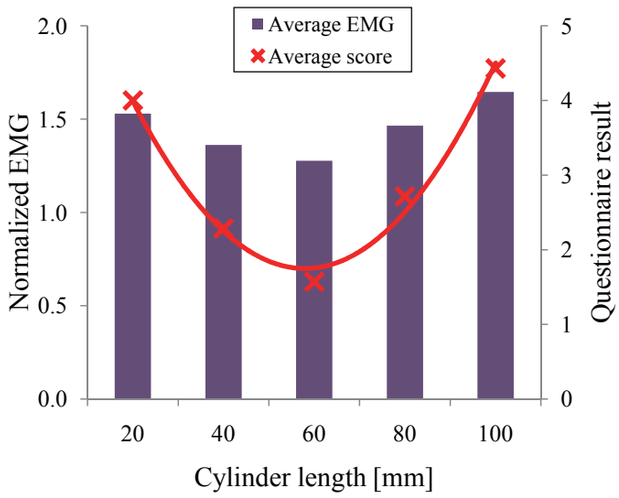

Fig. 12. Average EMG and questionnaire score (600[g])

quantitative evaluation using the muscle or tendon force. These results indicate a possibility that the quantitative evaluation using the muscle or tendon force.

3. Finger model

3.1 Tendon skeletal model

Fig. 13 shows the index finger and the thumb finger model. The index finger model consists of a fixed metacarpal and three phalanges. The DIP and PIP joints have 1 DOF (degree of freedom) for flexion/extension, and the MP joint has 2 DOF for flexion/extension and adduction/abduction. The thumb model contains a fixed trapezium bone and three phalanges. The IP joint has 1 DOF for flexion/extension, and the MP and CMC joints have 2 DOF for flexion/extension and adduction/abduction.

It is difficult to construct an anatomically accurate finger model because the human hand structure is very complex. Some research (Lee et al. (2008) and Deshpande et al. (2008))

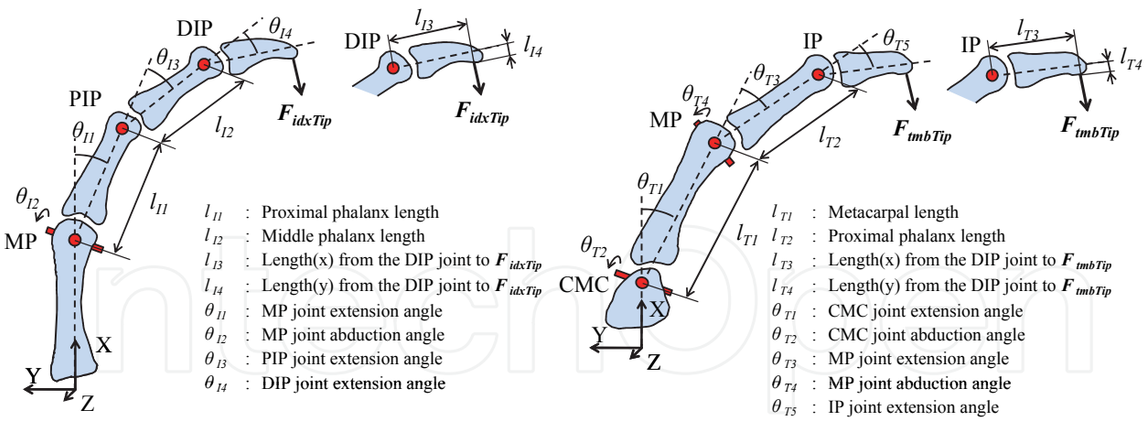

(a) Index finger model (b) Thumb model

Fig. 13. Index finger and thumb model

discussed the importance between the finger posture and the moment arm when exerting a fingertip force. Kamper et al. (2006) discussed importance of finger posture and moment arm when mapping from muscle activation to joint torque. The index finger joint torques $\boldsymbol{\tau}_{idx}$ and thumb joint torques $\boldsymbol{\tau}_{tmb}$ were calculated from the following equations:

$$\boldsymbol{\tau}_{idx} = \mathbf{M_{idx}}\mathbf{F_{idxTendon}} \tag{3}$$

$$\boldsymbol{\tau}_{tmb} = \mathbf{M_{tmb}}\mathbf{F_{tmbTendon}} \tag{4}$$

where $\boldsymbol{\tau}_{idx} = \left\{ \tau_{DIP}\ \tau_{PIP}\ \tau_{MCPa}\ \tau_{MCPf} \right\}^T$ is the vector of the index finger joint torques, $\mathbf{M_{idx}}$ is the matrix of the index finger moment arms at each joint, $\mathbf{F_{idxTendon}} = \left\{ f_{FDP}\ f_{FDS}\ f_{EIP}\ f_{EDC}\ f_{LUM}\ f_{DI}\ f_{PI} \right\}^T$ is the vector of the index finger tendon forces, $\boldsymbol{\tau}_{tmb} = \left\{ \tau_{IP}\ \tau_{MPa}\ \tau_{MPf}\ \tau_{CMCa}\ \tau_{CMCf} \right\}^T$ is the vector of the thumb joint torques, $\mathbf{M_{tmb}}$ is the vector of the thumb moment arms at each joint, and $\mathbf{F_{tmbTendon}} = \left\{ f_{FPL}\ f_{FPB}\ f_{EPL}\ f_{EPB}\ f_{APL}\ f_{APB}\ f_{ADPt}\ \ f_{ADPo}\ f_{OPP} \right\}^T$ is the vector of the thumb tendon forces.

3.2 Tendon moment arm

It is well known that the moment arm at each joint changes according to the joint angle. In this chapter, the moment arms $\mathbf{M_{idx}}$ and $\mathbf{M_{tmb}}$ are calculated by the quadratic approximation which is shown in Fig.14 and Fig.15. These profiles are given by the quadratic approximation based on the raw cadavers data that were measured by An et al. (1983) and Smutz et al. (1998). The tendon forces are calculated accurately using the variable moment arms.

3.3 Tendon force estimation

The joint torques $\boldsymbol{\tau}_{idx}$ and $\boldsymbol{\tau}_{tmb}$ can be calculated with Jacobian matrices:

$$\boldsymbol{\tau}_{idx} = \mathbf{J^T_{idx}}\mathbf{F_{idxTip}} \tag{5}$$

$$\boldsymbol{\tau}_{tmb} = \mathbf{J^T_{tmb}}\mathbf{F_{tmbTip}} \tag{6}$$

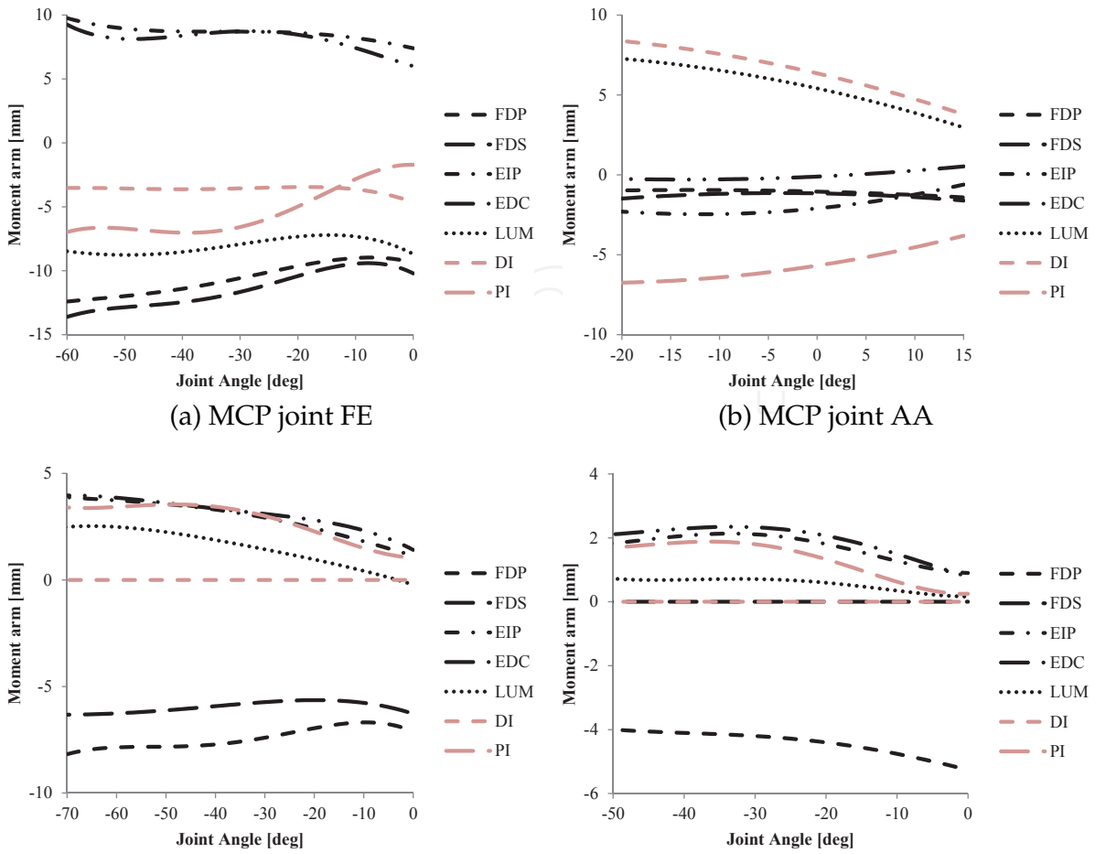

(a) MCP joint FE (b) MCP joint AA

(c) PIP joint FE (d) DIP joint FE

Fig. 14. Index finger moment arms

where $\mathbf{J_{idx}}$ is the index finger Jacobian matrix, $\mathbf{J_{tmb}}$ is the thumb Jacobian matrix, $\mathbf{F_{idxTip}} = \{ f_{Ix}\ f_{Iy}\ f_{Iz}\ \tau_{Ix}\ \tau_{Iy}\ \tau_{Iz} \}^T$ is the index fingertip force and torques, and $\mathbf{F_{tmbTip}} = \{ f_{Tx}\ f_{Ty}\ f_{Tz}\ \tau_{Tx}\ \tau_{Ty}\ \tau_{Tz} \}^T$ is the thumb fingertip force and torques. The following equations were obtained by substituting Eq. 3 to Eq. 6 (see definitions in Fig. 13):

$$\mathbf{F_{idxTip}} = \left(\mathbf{J_{idx}}\mathbf{J_{idx}^T}\right)^{-1}\mathbf{J_{idx}}\mathbf{M_{idx}}\mathbf{F_{idxTendon}} \tag{7}$$

$$\mathbf{F_{tmbTip}} = \left(\mathbf{J_{tmb}}\mathbf{J_{tmb}^T}\right)^{-1}\mathbf{J_{tmb}}\mathbf{M_{tmb}}\mathbf{F_{tmbTendon}}. \tag{8}$$

The tendon forces can be calculated from the fingertip forces based on Eq. 7 and Eq. 8. However, it is a redundant problem because 6 DOFs of the finger are driven by 7 tendons for the index finger, and 6 DOFs are driven by 9 tendons for the thumb. Therefore, the tendon

FDP	FDS	EIP	EDC	LUM	DI	PI	FPL	FPB	EPL	EPB	APL	APB	ADPt	ADPo	OPP
4.1	3.65	1.12	1.39	0.36	4.16	1.6	2.08	0.66	0.98	0.47	1.93	0.68	2.0	2.0	1.02

Table 3. PCSA (Physiological Cross Sectional Area) [cm^2] of each muscles (Valero-Cuevas et al. (1998) and Valero-Cuevas et al. (2003))

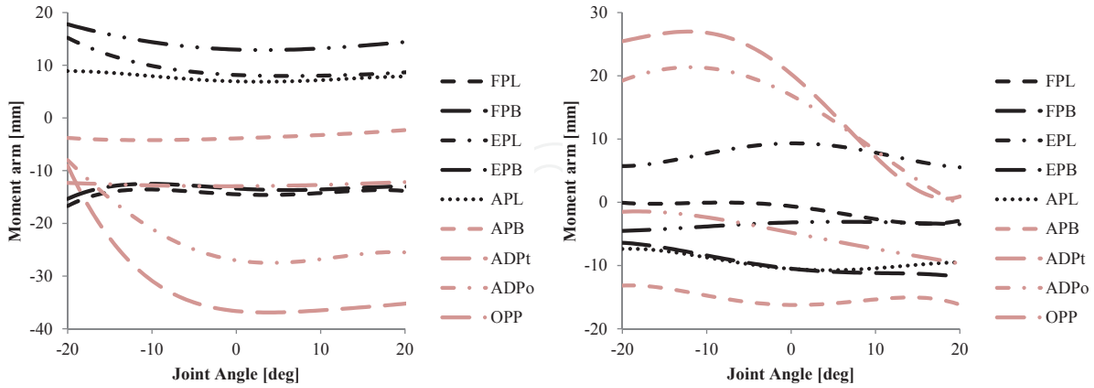

(a) CMC joint FE (b) CMC joint AA

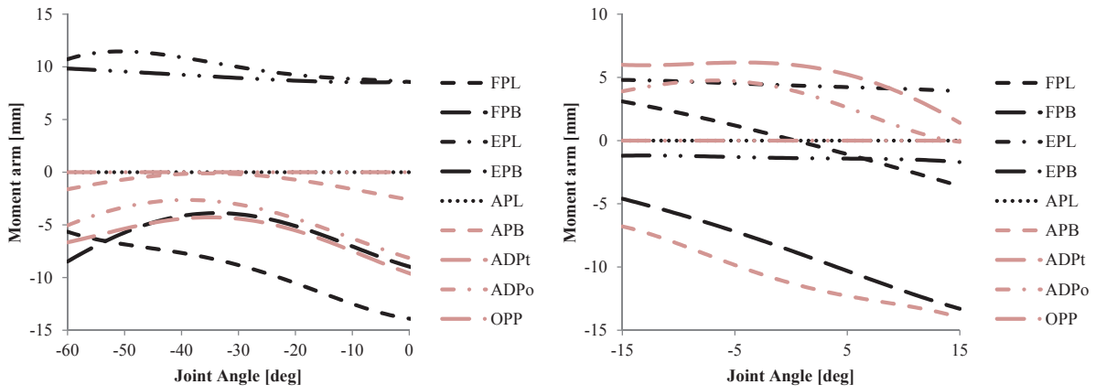

(c) MP joint FE (d) MP joint AA

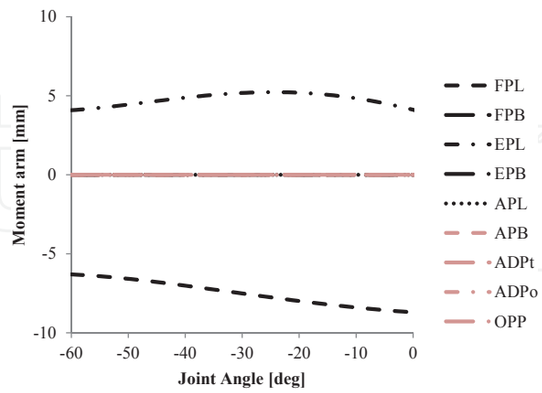

(e) IP joint FE

Fig. 15. Thumb moment arms

forces are derived by Crowninshield & Brand (1981) from the optimization calculation of the following equation:

$$u(F_{Tendon}) \triangleq \sum_{i=1}^{n} \left(\frac{f_i}{PCSA_i} \right)^2 \rightarrow \min \tag{9}$$

$$0 \leq f_i \leq f_{imax} \tag{10}$$

where $PCSA$ is a physiological cross sectional area of each muscle and f_{max} is a maximal force of each muscle that is determined by $PCSA$ and maximal muscle stress Zajac (1989). In this chapter, we used the $PCSA$ values of Cuevas *et al.* research Valero-Cuevas et al. (1998)Valero-Cuevas et al. (2003) (Table 3).

3.4 Score of the pinching effort

The pinching effort score is defined by following equation:

$$Score(F_{Tendon}) = \frac{1}{n} \sum_{i=1}^{n} \frac{f_i}{f_{imax}} \rightarrow \min \tag{11}$$

where n is the total number of tendons used for pinching an object. For example, when only the index finger used, n is 7, and when the index finger and the thumb used, n is 16. f_i is the tendon force of each tendon and f_{imax} is the maximum force that the muscle can exert to each tendon. The load ratio of each tendon f_i / f_{imax} denotes the force margin. Thus minimum score implies minimum load.

4. Cylinder pinching simulation

4.1 Condition of cylinder pinching simulation

Cylinder length 20, 40, 60, 80 or 100 [mm], diameter 20 [mm] and weight 600[g] are used in the simulation. The cylinder is pinched in the longitudinal direction by both the index finger and the thumb. Table 4 shows the finger model parameters and table 5 shows the limit angle of each joint. The finger link parameters are given based on the measurements of that of the subject. The contact points are the fingertip of each finger and the center of the cylinder. The friction coefficient is set as $\mu = 0.5$ and the fingertip force is set as 11.76 [N]. The vectors from the DIP/IP joint to the load point are $\mathbf{P_{idx}} = \left\{ 10.0\ 5.0\ 0.0 \right\}^T$ and $\mathbf{P_{tmb}} = \left\{ 17.0\ 5.0\ 0.0 \right\}^T$.

4.2 Simulation results of pinching cylinders

Fig. 16 shows the estimated tendon force for each of the index finger and the thumb when pinching the cylinders. The tendon forces of the thumb ADPt becomes higher according to the cylinder length. On the other hand, the tendon forces of the index finger FDS become lower according to the cylinder length. The pattern of these tendon forces is similar to the human muscle activity shown in Fig. 9 and Fig. 10. This suggests that the finger model can

l_{I1}	l_{I2}	l_{I3}	l_{I4}	l_{T1}	l_{T2}	l_{T3}	l_{T4}
39.0	25.0	10.0	5.0	45.0	32.0	17.0	5.0

Table 4. Finger link parameters [mm]

simulate the human muscle activity during the pinching activity. The score of each cylinder length was calculated from these tendon forces using Eq. 11.
Table 6 shows the simulated joint angles and measured joint angles of the human. In the simulation, the most efficient posture to exert fingertip force is when the AA directions of each joint are zero. The human finger postures are different from the simulation results (see θ_{I2} and θ_{T2} in table 6). This comes from the modeling and measurement errors. However, there are strong correlations between the simulated joint angles and the measured joint angles. Table 7 shows the correlation coefficients and p-value when pinching the 20 to 100 [mm] cylinder respectively. The average error of all the joint angles is 5.86 [deg] and the standard deviation of the error is 4.40 [deg]. These results show that the estimated finger posture is sufficient for pinching force estimation.

	flexion(adduction)	extension(abduction)
θ_{I1} [degree]	-60	0
θ_{I2} [degree]	-25	15
θ_{I3} [degree]	-75	0
θ_{I4} [degree]	-60	0

	flexion(adduction)	extension(abduction)
θ_{T1} [degree]	-20	25
θ_{T2} [degree]	-20	20
θ_{T3} [degree]	-60	10
θ_{T4} [degree]	-15	15
θ_{T5} [degree]	-60	20

Table 5. Limit angles of each joint

Cylinder length	θ_{I1}	θ_{I2}	θ_{I3}	θ_{I4}
20 [mm]	-60.0	0.0	-18.5	-11.9
40 [mm]	-51.2	0.0	-24.3	-17.0
60 [mm]	-37.8	0.0	-20.7	-21.5
80 [mm]	-19.5	0.0	-25.6	-26.5
100 [mm]	-2.3	0.0	-19.4	-29.7

Cylinder length	θ_{I1}	θ_{I2}	θ_{I3}	θ_{I4}
20 [mm]	-62.5	-6.8	-23.6	-5.6
40 [mm]	-51.6	-4.8	-27.0	-9.5
60 [mm]	-21.8	-0.6	-15.9	-17.6
80 [mm]	-8.1	-3.2	-18.3	-23.6
100 [mm]	14.2	-7.1	-17.3	-31.2

Cylinder length	θ_{T1}	θ_{T2}	θ_{T3}	θ_{T4}	θ_{T5}
20 [mm]	-3.8	0.0	-3.0	0.0	-5.1
40 [mm]	4.0	0.0	-10.1	0.0	-7.2
60 [mm]	5.1	0.0	-0.1	0.0	-11.0
80 [mm]	9.3	0.0	-4.9	0.0	-11.2
100 [mm]	14.4	0.0	-3.1	0.0	10.8

Cylinder length	θ_{T1}	θ_{T2}	θ_{T3}	θ_{T4}	θ_{T5}
20 [mm]	-4.5	8.5	-5.0	-	-
40 [mm]	0.4	14.8	-10.6	-	-
60 [mm]	12.3	-1.8	-10.6	-	-
80 [mm]	16.3	-7.3	-10.6	-	-
100 [mm]	15.5	-11.7	-11.0	-	-

Table 6. Simulated and measured joint angle ([deg])

	20 [mm]	40 [mm]	60 [mm]	80 [mm]	100 [mm]
Correlation coefficient	0.98	0.96	0.87	0.85	0.83
P-value	$\ll$0.001	$<$0.001	0.012	0.016	0.020

Table 7. The correlation coefficient of the joint angles

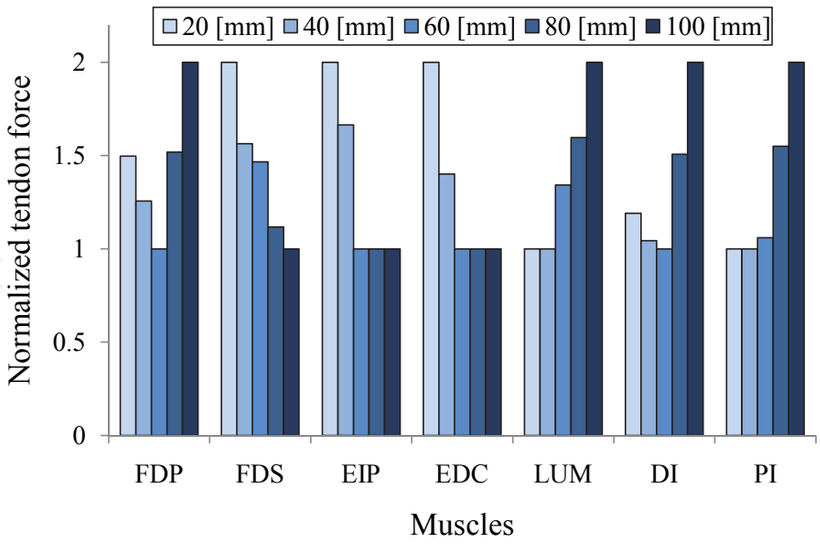

(a) Muscle of the index finger

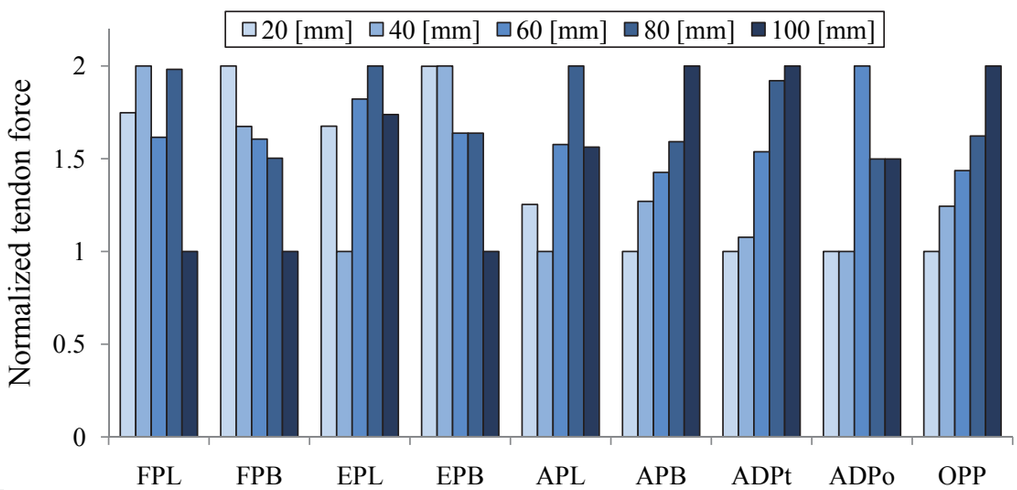

(b) Muscle of the thumb

Fig. 16. Simulation results

Fig. 17 shows the evaluated score by the simulation and human questionnaire results. The curves in the figure are the approximate quadratic curve of the results. The lowest score is observed in the 60 [mm] cylinder length. On the other hand, the highest score is observed in the 20 [mm] cylinder length. The simulated score pattern is similar to the human questionnaire score pattern. There is a strong correlation between the simulated score and the questionnaire score of human (the correlation coefficient is 0.97 and the p-value is 0.007). This indicates that the proposed method can reflect the human subjective pinching effort and our finger model is useful for the pinching effort evaluation.

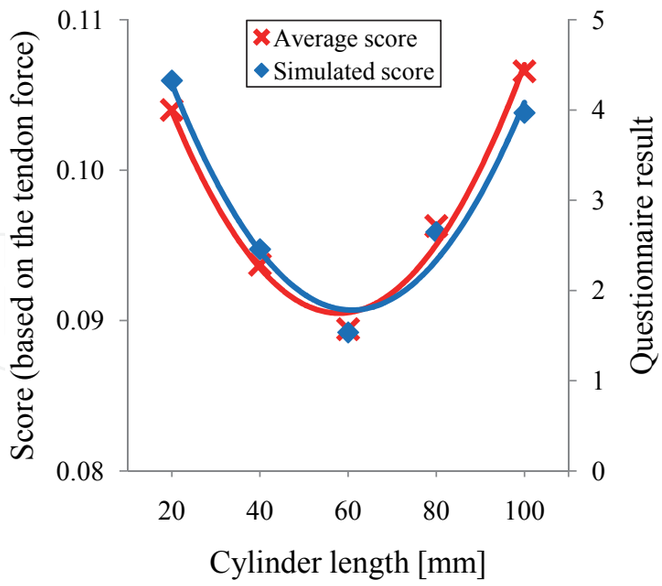

Fig. 17. Simulation scores

5. Conclusion

This research is aimed at the quantification of the product usability based on the estimated tendon force. At the first step of the quantitative evaluation, we tried to evaluate a pinching activity. We proposed the evaluation method of the pinching effort and show the effectiveness of the proposed method.

At first, we showed the importance of the tendon forces to evaluate pinching effort by human experiment. The experimental results of a human pinching a cylinder are shown: the subjective pinching effort, the pinching force, the human EMG, and the finger posture. These experimental results indicate that the integrated surface EMG is one of the important indexes to indicate pinching effort. This suggests a possibility for quantitative evaluation using the muscle or tendon force. Second, the index finger and thumb models that are used for the tendon force estimation are developed. The finger models mimic the human tendon skeletal structure. The simulation results of the pinching activity are compared with the sensory evaluation of subjects. The experimental results show that the simulation scores are similar to the questionnaire survey results and the estimated finger posture is also similar to the human finger posture. Our method can evaluate the pinching effort from the viewpoint of the muscle activity.

6. References

An, K. N., Chao, E. Y., Cooney, W. P. & Linscheid, R. L. (1979). Normative model of human hand for biomechanical analysis, *Journal of Biomechanics* 12(10): 775–88.

An, K. N., Ueba, Y., Chao, E. Y., Cooney, W. P. & Linscheid, R. L. (1983). Tendon excursion and moment arm of index finger muscles, *Journal of Biomechanics* 16(6): 419–25.

Brook, N., Mizrahi, J., Shoham, M. & Dayan, J. (1995). A biomechanical model of index finger dynamics, *Medical Engineering & Physics* 17(1): 54 – 63.

Crowninshield, R. D. & Brand, R. A. (1981). A physiologically based criterion of muscle force prediction in locomotion, *Journal of Biomechanics* 14(11): 793–801.

Deshpande, A. D., Balasubramanian, R., Lin, R., Dellon, B. T. & Matsuoka, Y. (2008). Understanding variable moment arms for the index finger mcp joints through the act hand, *The second IEEE/RAS-EMBS International Conference on Biomedical Robotics and Biomechatronics (BioRob2008)*, pp. 776–82.

Flanagan, J. R., Bowman, M. C. & Johansson, R. S. (2006). Control strategies in object manipulation tasks, *Current Opinion in Neurobiology* 16(6): 650–9.

Holzbaur, K. R. S., Murray, W. M. & Delp, S. L. (2005). A model of the upper extremity for simulating musculoskeletal surgery and analyzing neuromuscular control, *Annals of Biomedical Engineering* 33(6): 829–40.

Ikeda, A., Kurita, Y. & Ogasawara, T. (2008). Pinching motion evaluation using human like sensing device, *Proceedings of Joint 4th International Conference on Soft Computing and Intelligent Systems and 9th International Symposium on advanced Intelligent Systems (SCIS & ISIS 2008)*, pp. 1135–8.

Ikeda, A., Kurita, Y. & Ogasawara, T. (2009a). Evaluation of pinching effort by a tendon-driven robot hand, *Proceedings of 2009 IEEE International Conference on Robotics and Automation (IEEE ICRA 2009)*, pp. 3437–42.

Ikeda, A., Kurita, Y. & Ogasawara, T. (2009b). A tendon skeletal finger model for evaluation of pinching effort, *Proceedings of 2009 IEEE/RSJ International Conference on Intelligent Robots and Systems (IEEE IROS 2009)*, pp. 3691–6.

Kamper, D. G., Fischer, H. C. & Cruz, E. G. (2006). Impact of finger posture on mapping from muscle activation to joint torque, *Clinical Biomechanics* 21(4): 361–9.

Kong, Y. K. & Freivalds, A. (2003). Evaluation of meat-hook handle shapes, *International Journal of Industrial Ergonomics* 32(2): 13–23.

Lee, S. W., Chenb, H., Towlesa, J. D. & Kamper, D. G. (2008). Estimation of the effective static moment arms of the tendons in the index finger extensor mechanism, *Journal of Biomechanics* 41(7): 1567–73.

Nakamura, Y., Yamane, K., Fujita, Y. & Suzuki, I. (2005). Somatosensory computation for man-machine interface from motion capture data and musculoskeletal human model, *IEEE Transactions on Robotics* 21(1): 58–66.

Radhakrishnan, S. & Nagaravindra, M. (1993). Analysis of hand force in health and disease during maximum isometric grasping of cylinders, *Medical and Biological Engineering and Computing* 31(4): 372–6.

Smutz, W. P., Kongsayreepong, A., Hughes, R. E., Niebur, G., Cooney, W. P. & An, K. N. (1998). Mechanical advantage of the thumb muscles, *Journal of Biomechanics* 31(6): 565–70.

Sueda, S., Kaufman, A. & Pai, D. K. (2008). Musculotendon simulation for hand animation, *ACM Transactions on Graphics (Proceedings SIGGRAPH)* 27(3): 775–88.

Tada, M. & Pai, D. K. (2008). Finger shell: Predicting finger pad deformation under line loading, *Proceedings of the Symposium on Haptic Interfaces for Virtual Environment and Teleoperator Systems*, pp. 107–112.

Valero-Cuevas, F. J. (2005). An integrative approach to the biomechanical function and neuromuscular control of the fingers, *Journal of Biomechanics* 38(4): 673–84.

Valero-Cuevas, F. J., Johanson, M. E. & Towles, J. D. (2003). Towards a realistic biomechanical model of the thumb: the choice of kinematic description may be more critical than

the solution method or the variability/uncertainty of musculoskeletal parameters, *Journal of Biomechanics* 36(7): 1019–30.

Valero-Cuevas, F. J., Zajac, F. E. & Burgar, C. G. (1998). Large index-fingertip forces are produced by subject-independent patterns of muscle excitation, *Journal of Biomechanics* 31(8): 693–703.

Zajac, F. E. (1989). Muscle and tendon: properties, models, scaling, and application to biomechanics and motor control, *Biomedical Engineering* 17(4): 359–411.

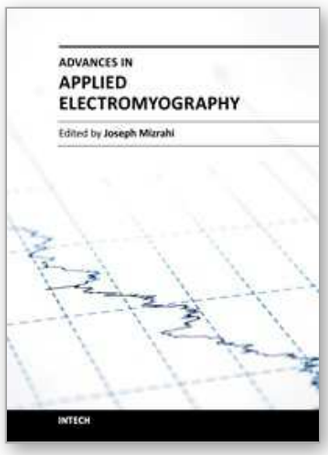

Advances in Applied Electromyography
Edited by Prof. Joseph Mizrahi

ISBN 978-953-307-382-8
Hard cover, 212 pages
Publisher InTech
Published online 29, August, 2011
Published in print edition August, 2011

The electrical activity of the muscles, as measured by means of electromyography (EMG), is a major expression of muscle contraction. This book aims at providing an updated overview of the recent developments in electromyography from diverse aspects and various applications in clinical and experimental research. It consists of ten chapters arranged in four sections. The first section deals with EMG signals from skeletal muscles and their significance in assessing biomechanical and physiologic function and in applications in neuro-musculo-skeletal rehabilitation. The second section addresses methodologies for the treatment of the signal itself: noise removal and pattern recognition for the activation of artificial limbs. The third section deals with utilizing the EMG signals for inferring on the mechanical action of the muscle, such as force, e.g., pinching force in humans or sucking pressure in the cibarial pump during feeding of the hematophagous hemiptera insect. The fourth and last section deals with the clinical role of electromyograms in studying the pelvic floor muscle function.

INTECH
open science | open minds

InTech Europe
University Campus STeP Ri
Slavka Krautzeka 83/A
51000 Rijeka, Croatia
Phone: +385 (51) 770 447
Fax: +385 (51) 686 166
www.intechopen.com

InTech China
Unit 405, Office Block, Hotel Equatorial Shanghai
No.65, Yan An Road (West), Shanghai, 200040, China
中国上海市延安西路65号上海国际贵都大饭店办公楼405单元
Phone: +86-21-62489820
Fax: +86-21-62489821

IntechOpen